

TT Ari and its Quasi-Periodic Oscillations

J. S m a k

N. Copernicus Astronomical Center, Polish Academy of Sciences,
Bartycka 18, 00-716 Warsaw, Poland
e-mail: jis@camk.edu.pl*Received*

ABSTRACT

Quasi-periodic oscillation (QPO) of TT Ari are transient, short-living phenomena. They appear and disappear and their periods and amplitudes vary on a time scale as short as 1 hour. Consequently the periodograms covering longer intervals of time are generally meaningless.

Key words: *binaries: cataclysmic variables, stars: individual: TT Ari*

1. Introduction

TT Ari is a nova-like cataclysmic variable showing several types of variability (cf. Smak 2013 and references therein). Among them are: (1) negative superhumps with $P \approx 0.1329$ d, and full amplitude $2A \approx 0.2$ mag., often referred to as "3-hour" variations, and (2) transient, quasi-periodic oscillations (QPO's) with periods between 10 and 40 minutes and full amplitudes up to $2A \approx 0.2$ mag.

In spite of numerous investigations the evidence concerning the nature and characteristics of those QPO's is confusing:

Williams (1966) from the analysis of one particular night found three QPO's being present in the second part of this run, but absent in its first part.

Semeniuk et al. (1987) calculated global periodograms for several seasons and found just one persistent QPO, its period decreasing from $P_{QPO} \approx 27$ min in 1961/62 to $P_{QPO} \approx 17$ min in 1985.

Many authors (e.g. Andronov 1999, Kim 2009, Kraicheva et al. 1997,1999, Tremko et al. 1996, Udalski 1987) found several QPO's, with periods in the range $P_{QPO} \sim 10 - 40$ minutes, being often simultaneously present in the periodograms based on a single night or in global periodograms based on a given season.

Vogt et al. (2013) analyzed the continuous 10-day light curve obtained in 2007 with the MOST satellite and found *no* QPO in the global periodogram in the range from 10 to 30 minutes and amplitude exceeding 0.25 percent.

The purpose of the present paper is to clarify this situation by presenting results of a more detailed analysis of the behavior of individual QPO's.

2. The Data

The data used in the present investigation consist of 15 light curves (4 in V and 11 in U) collected by the author in 1961/62 at the Lick Observatory and in 1966 at the Observatoire de Haute Provence (see Smak 2013); they are identified in the first two columns of Table 1 below. The duration of those runs was from 2 to 5 hours.

Prior to further analysis variations related to the negative superhumps were removed, using periods P_{nSH} applicable to a given season and amplitudes A_{nSH} applicable to a given night. Examples of such "pre-whitened" light curves were shown in the previous paper (Smak 2013, Figs.1 and 3).

3. The QPO Periods and Amplitudes

We begin by calculating periodograms. Each run is divided into two parts and three periodograms, covering periods from 5 to 60 minutes, are calculated separately for those two parts and for the entire run. In what follows we shall refer to them as "part 1", "part 2", and "both parts", with corresponding QPO periods and amplitudes being designated as $P(1)$, $P(2)$, $P(1+2)$ and $A(1)$, $A(2)$, $A(1+2)$.

Examples of periodograms are shown in Fig.1 to illustrate their main characteristics: (1) periodograms for part 1, part 2, and both parts are generally different, and (2) different periodicities are present in periodograms obtained from different nights.

To determine the QPO periods and amplitudes we proceed in the usual way: After finding the period and amplitude of the strongest QPO present in the periodogram we pre-whiten the light curve by subtracting this strongest signal and calculate the next periodogram. The procedure is repeated until no signal with amplitude exceeding of 0.03 mag. can be seen in the periodogram. This particular limit was set arbitrarily. Additional calculations showed, however, that making it lower would result in adding only few weaker periodicities not affecting our main conclusions.

Results are listed in Table 1, where periods are given in minutes and amplitudes – in magnitudes, and the histogram of periods $P(1)$ and $P(2)$ contained in that table is shown in Fig.2. Those results can be summarized in the following points: (a) The QSO amplitudes in U are larger than in V. (b) The amplitudes $A(1+2)$ are lower than $A(1)$ and $A(2)$. (c) The QSO periods show concentration between 10 and 40 days. There are only two cases with periods shorter than 10 minutes (9.8 and 8.9 min.) and few periods longer than 40 minutes. (d) In about 50 percent of cases there are two or more QPO periods being simultaneously present in a given part. (e) The periods present in the two parts are generally different. There are only 6

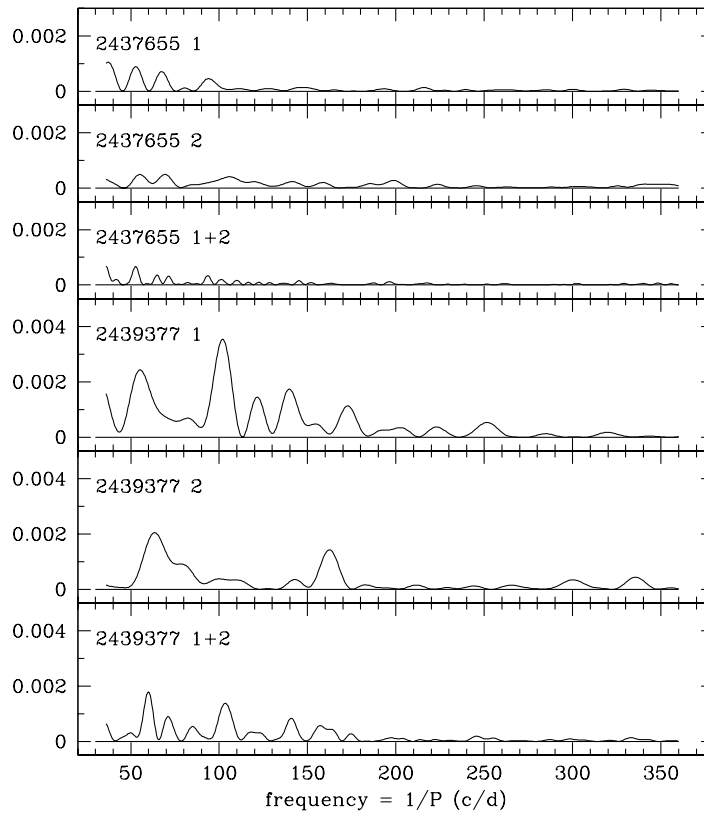


Fig. 1. Examples of periodograms calculated separately for the two parts of a given run and for the entire run (1+2).

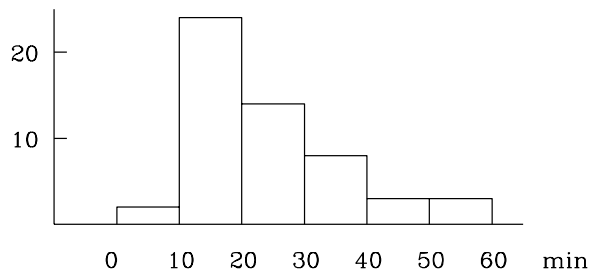


Fig. 2. Histogram of QPO periods from part 1 and part 2 contained in Table 1.

cases with pairs of $P(1)$ and $P(2)$ (shown in Table 1 in boldface) differing by less than 2 days. (f) There are only 11 cases with $P(1+2)$ being within 2 days of $P(1)$ or $P(2)$. (g) The 3 QPO periods obtained for the second part of JD 2437679 differ slightly from those obtained by Williams (1966), most likely due to the fact that

Table 1
QPO Periods and Amplitudes

2430000+	C	P(1)	A(1)	P(2)	A(2)	P(1+2)	A(1+2)
7646	V	18.0	0.038	19.6	0.032	19.1	0.033
7655	V	38.8	0.032
		21.1	0.030
7656	V	16.8	0.029
7660	V	12.1	0.036
7660	U	16.2	0.048	13.4	0.040
		41.1	0.040
7664	U	38.6	0.037	17.3	0.032
		20.4	0.031
7672	U	50.0	0.054	16.1	0.083	15.4	0.062
		29.0	0.050	37.2	0.070	24.4	0.059
		20.7	0.037	9.8	0.040
7675	U	23.3	0.070	57.3	0.051	25.7	0.040
		21.9	0.040	20.2	0.034
7679	U	17.5	0.041
		14.1	0.037
		37.9	0.034
7692	U	35.1	0.056	13.9	0.043	19.4	0.035
		12.5	0.044	10.7	0.031	11.8	0.032
		20.1	0.030	29.7	0.031
9360	U	26.8	0.051	30.3	0.033
		36.1	0.040	25.7	0.030
9375	U	38.0	0.054	18.5	0.054	18.5	0.040
		26.6	0.038	22.5	0.044	24.3	0.037
		14.2	0.038	38.4	0.030
9376	U	11.7	0.030
		31.3	0.047	18.4	0.030	14.0	0.034
		13.6	0.043	14.5	0.032
9377	U	43.5	0.032
		14.1	0.059	22.7	0.045	24.0	0.042
		25.5	0.044	8.9	0.037	13.9	0.037
9378	U	53.1	0.039
		10.4	0.034
		15.2	0.052	15.4	0.046	19.9	0.044
		20.3	0.045	19.1	0.046	15.8	0.043
		28.5	0.036	48.8	0.032	14.6	0.032

he used incorrect value of P_{nSH} (0.1171 instead of 0.1329 d). (h) No relation was found between the presence (or absence) of QPO's and the negative superhump phase, the orbital phase, or the beat phase.

Using those results we can conclude that (1) the QPO's are short-living phenomena, (2) two or more QPO's can be simultaneously present, and (3) the periodicities present in periodograms obtained for "both parts" are either due to a strong QPO present in part 1 or part 2, or are artifacts unrelated to $P(1)$ or $P(2)$. We shall return to some of those points and strengthen those conclusions in the next Section.

4. The QPO Light Curves

We now turn to QPO light curves. For a specific QPO period P_{QPO} the original light curve (pre-whitened with P_{nSH} ; see Section 2) is pre-whitened with all other QPO periodicities. Then a series of *composite* light curves with P_{QPO} are constructed, each of them including data points from 3 cycles, and each consecutive curve being shifted with respect to the previous one by one cycle. Two such series of composite light curves are shown, as examples, in Fig.3. The periods used in those two cases are the strongest periods detected in the periodograms: $P(2) = 16.1$ min. in JD 2437672 and $P(1) = 23.3$ min. in JD 2437675.

As can be seen from Fig.3 the QPO amplitudes vary on a short time scale. In addition the curves are shifted in phase what is an obvious indication of period variations. To study those variations in more details we proceed as follows. For each light curve a cosine curve is fitted to the points giving the amplitude A_{QSO} and the phase of maximum ϕ_{max} . Those two parameters are then plotted as functions of time. Eight representative examples of the resulting ϕ_{max} vs. time and A_{QSO} vs. time plots are shown in Figs.4-6 and discussed below. Note that the ϕ_{max} vs. time plots are equivalents of the ($O - C$) diagrams.

JD 2437672 (Figs.3 and 4a). The QPO with $P(2) = 16.1$ min. detected in part 2 was actually present also in part 1. Its amplitude was initially very low, increased on a time scale of ~ 1 hour, reaching maximum at JD 2437672.66 and beginning to decrease afterwards. The period increased at a high rate: $dP/dt = +0.054 \pm 0.018$.

JD 2437675 (Figs.3 and 4b). The QPO with $P(1) = 23.3$ min. detected in part 1 had originally record high amplitude: $A \approx 0.11$ mag. It decreases rapidly, however, and after few cycles (or about 1 hour) it practically disappeared. The period decreased at a high rate: $dP/dt = -0.074 \pm 0.014$.

JD 2437692 (Fig.4c). Two QPO's present in part 1 and part 2 had close periods: $P(1) = 12.5$ and $P(2) = 13.9$ min. Our analysis performed with the mean value $P = 13.2$ min shows that this was the same QPO with rapidly increasing period ($dP/dt = +0.038 \pm 0.012$) and roughly constant amplitude. Regretably, this was the shortest run covering only 2 hours.

JD 2439375 (Fig.5a). Three periods detected in the periodogram: $P(1) = 26.6$, $P(2) = 22.5$, and $P(1+2) = 24.3$ min. are close to $P = 24$ min found by Semeniuk

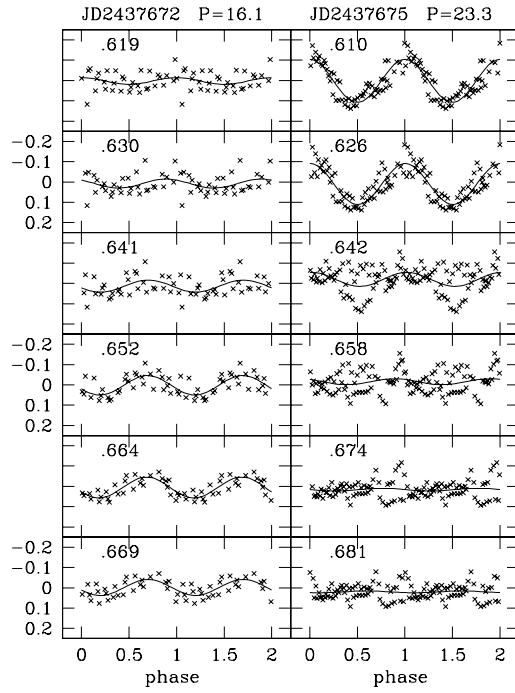


Fig. 3. Composite light curves of QSO's with $P = 16.1$ min on JD 2437672 (*left*) and $P = 23.3$ min on JD 2437675 (*right*). Each curve includes 3 cycles and is shifted with respect to the previous one by one cycle. Solid lines represent the best fit cosine curves. See text for details.

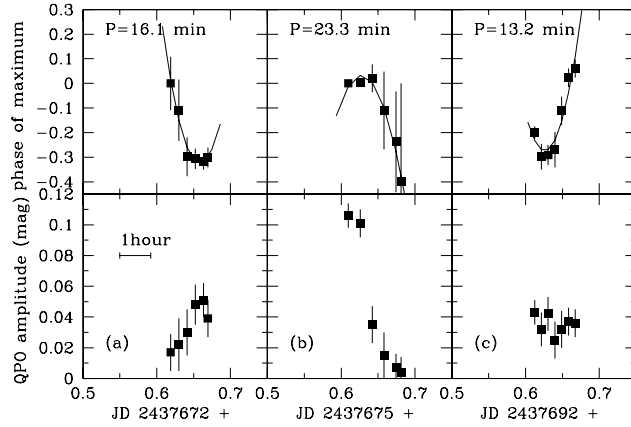


Fig. 4. Variability of periods and amplitudes of three QPO's observed on JD 2437672, JD 2437675 and JD 2437692. Solid lines are the best fit parabolas describing period variations. See text for details.

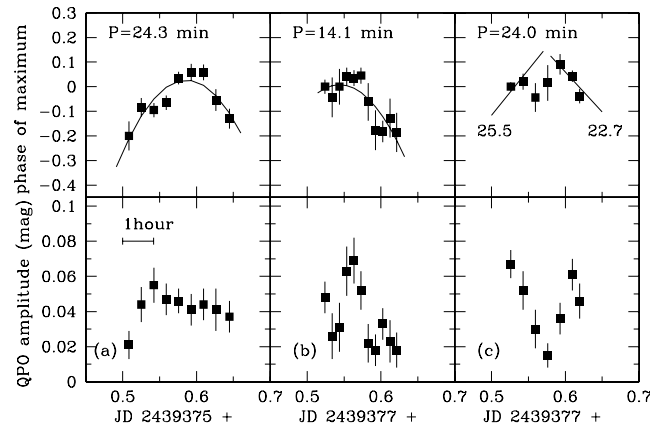


Fig. 5. Variability of periods and amplitudes of three QPO's observed on JD 2439375 and JD 2439377. Solid lines represent the best fit cosine curves. Short lines in (c) represent periods identified in the periodograms. See text for details.

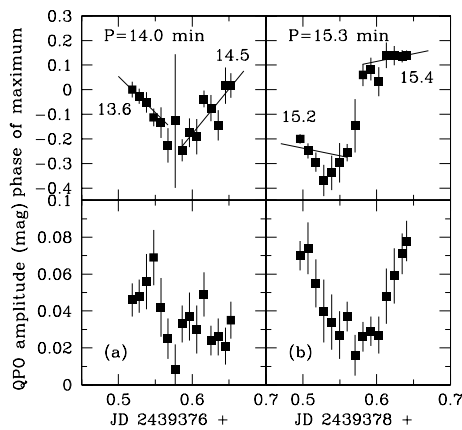


Fig. 6. Variability of periods and amplitudes of QSO's observed on JD 2439376 and JD 2439378. Short lines represent periods identified in the periodograms. See text for details.

et al. (1987) in their global periodogram. Results of the analysis performed with $P = 24.3$ min show (Fig.5a) that this was one QPO with rapidly decreasing period ($dP/dt = -0.022 \pm 0.005$).

JD 2439377 (Fig.5b). The QPO with $P(1) = 14.1$ min. detected in part 1 was actually a short living feature with amplitude growing to maximum near JD 2439377.56, lasting for less than 1 hour, and then decreasing. The period decreased at a rate: $dP/dt = -0.007 \pm 0.004$.

JD 2439377 (Fig.5c). Three periods detected in the periodogram: $P(1) = 25.5$, $P(2) = 22.7$, and $P(1+2) = 24.0$ min. are close to $P = 24$ min detected by Semeniuk et al. (1987) in their global periodogram. Results of the analysis performed with $P = 24.0$ min show (Fig.5c) that there were two different QPO's. The first, with $P = 25.5$, rapidly declined in amplitude and near *JD 2439377.57* was replaced by another one with $P(2) = 22.7$ and rapidly growing amplitude. Therefore the period $P = 24$ min was an artifact unrelated to the two real periodicities.

JD 2439376 (Fig.6a). Two QPO present in part 1 and part 2 had close periods: $P(1) = 13.6$ and $P(2) = 14.5$ min. Results of the analysis performed with the mean value $P = 14.0$ min (Fig.6a) could – at first sight – suggest that this was the same QPO with rapidly increasing period. One should note, however, that the amplitude, after reaching maximum near *JD 2439376.55*, declined rapidly and around *JD 2439376.575* the QPO with $P = 13.6$ disappeared, being replaced by another one with $P(2) = 14.5$. The two solid lines represent periods $P(1) = 13.6$ and $P(2) = 14.5$ min. Note that they were nearly constant.

JD 2439378 (Fig.6b). This is another example of two strong QPO present in part 1 and part 2 having close periods: $P(1) = 15.2$ and $P(2) = 15.4$ min. Results of the analysis performed with the mean value $P = 15.3$ min (Fig.6b) are unambiguous: A large jump in ϕ_{max} clearly shows that there were two different QPO's. The first QPO with $P = 15.2$ rapidly declined in amplitude and near *JD 2439378.57* was replaced by another one with $P(2) = 15.4$ and rapidly growing amplitude. The two solid lines represent periods $P(1) = 15.2$ and $P(2) = 15.4$ min. Note that they were variable: $P(1)$ – increasing and $P(2)$ – decreasing.

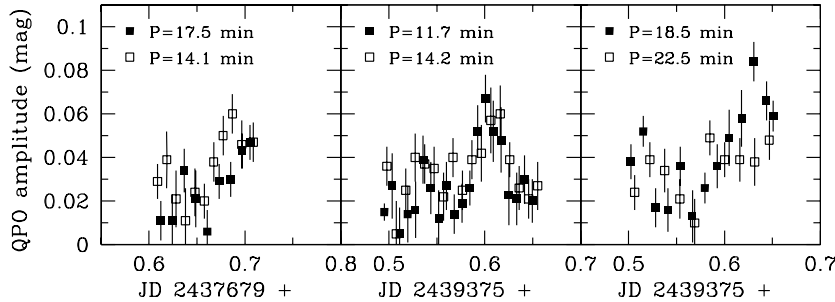


Fig. 7. Variability of QSO amplitudes observed simultaneously on *JD 2437679* and *JD 2439375*.

The A_{QSO} vs. time plots permit also to check whether multiple QPO's identified in the periodograms were indeed present simultaneously. Fig.7 shows the amplitudes of two QPO's detected in part 2 of *JD 2437679* and of four QPO's in part 2 of *JD 2439375*. In both cases the QPO amplitudes varied in a similar way, on a time scale of ~ 1 hour, reaching their maxima simultaneously or nearly simultaneously.

5. Discussion

The most important result of the present investigation is that the quasi periodic oscillations of TT Ari are transient, short-living phenomena which appear and disappear on a time scale as short as 1 hour. Their amplitudes and periods are strongly variable on a similar, very short time scale.

The obvious consequence of this behavior is that periodograms calculated from data covering longer intervals of time, particularly global periodograms covering the entire season, only seldom can show real periodicities, but – generally – are meaningless. This is best illustrated by the global periodogram obtained by Vogt et al. (2013, Fig.3) from data covering 10 days: it did not show *any* QPO's with amplitude exceeding 0.0025 mag. On the other hand, however, their light curves (Vogt et al. 2013, Fig.1) showed clearly many transient QPO's with full amplitudes 2A up to 0.1 mag. (for example, there was a strong QPO with $P \approx 23$ min on JD 2454404).

The nature and origin of QPO's in TT Arietis remain unclear...

REFERENCES

- Andronov, I.L., Arai, K., Chinarova, L.L., Dorokhov, N.I., Dorokhova, T.N., Dumitrescu, A., Nogami, D., Kolesnikov, S.V., Lepardo, A., Mason, P.A., Matsumoto, K., Oprescu, G., Pajdosz, G., Passuelo, R., Patkos, L., Senio, D.S., Sostero, G., Suleimanov, V.F., Tremko, J., Zhukov, G.V., Zoła, S. 1999, *AJ*, **117**, 574.
- Kim, Y., Andronov, I.L., Cha, S.L., Chinarova, L.L., Yoon, J.N. 2009, *A&A*, **496**, 765.
- Kraicheva, Z., Stanishev, V., Iliev, L., Antonov, A., Genkov, V. 1997, *A&ASuppl.Ser.*, **122**, 123.
- Kraicheva, Z., Stanishev, V., Genkov, V., Iliev, L. 1999, *A&A*, **351**, 607.
- Semeniuk, I., Schwarzenberg-Czerny, A., Duerbeck, H., Hoffman, M., Smak, J., Stępień, K., Tremko, J. 1987, *Acta Astron.*, **37**, 197.
- Smak, J. 2013, *Acta Astron.*, **63**, 453.
- Tremko, J., Andronov, I.L., Chinarova, L.L., Kumsiashvili, M.I., Luthardt, R., Pajdosz, G., Patkósz, L., Röbinger, S., Zoła, S. 1996, *A&A*, **312**, 121.
- Udalski, A. 1988, *Acta Astron.*, **38**, 315.
- Vogt, N., Chené, A.-N., Moffat, A.F.J., Matthews, J.M., Kuschnig, R., Guenther, D.B., Rowe, J.F., Ruciński, S., Sasselov, D., Weiss, W.W. 2013, *Astronomische Nachrichten*, **334**, 1101.
- Williams, J.O. 1966, *PASP*, **78**, 279.